 doi:10.20944/preprints202209.0138.v1

Article

Uranium(VI) retention onto hardened cement paste under high saline and alkaline conditions

Nathalie Macé [1]*, Jacques Page [1] and Pascal E. Reiller [2]

[1] - Université Paris-Saclay, CEA, Service d'Etude du Comportement des Radionucléides, 91191, Gif-sur-Yvette, France
[2] - Université Paris-Saclay, CEA, Service d'Etudes Analytiques et de Réactivité des Surfaces, 91191, Gif-sur-Yvette, France
* Correspondence: nathalie.mace@cea.fr; Tel.: +33 1 69 08 32 38

Abstract: Evaluation of the mobility behavior of radionuclides in highly saline and alkaline conditions is a major concern for performance assessment of radioactive waste disposal. The aim of this study is to determine the effect of up to 2.8 mol/$kg_{solution}$ content of $NaNO_3$, onto the solubility and the sorption of U(VI) in a hardened cement-paste (HCP) prepared from an ordinary Portland cement (CEM I). To avoid the interference of the high salt concentration (and ionic strength) and because of expected low solubility of uranium under such alkaline conditions, the time-resolved laser fluorescence (TRLFS) was selected to measured accurate U(VI) concentration in solution using the standard addition method in 85% H_3PO_4 to limit dilution and matrix effects and allows determining of resulting [U(VI)] in solution with acceptable precision for distribution factor (R_d) both in sorption and desorption experiments. The operational solubility limit measured at high ionic strength is lowered by a factor 3 compared to the reference cementitious condition, with the R_d values decrease by *ca.* a factor 4. Sorption of U(VI) appears to be reversible under these conditions.

Keywords: radionuclide, uranyl, retention, cementitious media, saline plume, $NaNO_3$, luminescence, TRLFS

1. Introduction

In the framework of radioactive waste disposal, the French national agency for radioactive waste management (Andra) managed the CTEC laboratory group project dedicated to evaluate the behavior of radionuclides (RN) and toxic species in complex environments, particularly in highly saline and alkaline conditions. Some intermediate-level long-lived (ILW-LL) wastes are supposed to contain high levels of soluble salts, mainly composed of sodium nitrate ($NaNO_3$) and sodium sulfate (Na_2SO_4) in contact with cement-based materials, such as concrete, mortars, or grouts. Such alkaline and saline plume could therefore induce changes in RN speciation and mobility in parallel with significant changes in the mineralogical assembly and thermodynamic equilibria.

In alkaline media and at ionic strength up to 250 mM, solubility limit of U(VI) is expected to be low and its retention in cement based material can be very high [1]. Calcium uranate ($CaUO_4$(cr)) calcium diuranate ($CaU_2O_7 3H_2O$(cr)), sodium diuranate ($Na_2U_2O_7$), or uranophane ($Ca(UO_2)_2(SiO_3OH)_2{:}5H_2O$) are U(VI) containing solid phases that are relevant to determine the solubility limit of uranium (*e.g.* [2-5]). Recent data [6-8] concerning U(VI)-solubility limiting phase in high saline media containing NaCl and/or KCl also evidenced $UO_3{:}2H_2O$(cr), $K_2U_6O_{19}{:}11H_2O$, $K_2U_2O_7{:}1.5H_2O$, and $Na_2U_2O_7{:}H_2O$. These phases can be then used to describe and predict the U(VI) solubility in various cementitious media.

Concerning the evolution of mineralogical assembly of cement-based materials in highly saline conditions, numerous data in literature exists – see *e.g.* [9-12]. For ionic strength higher that 4 mol/kg_{water} thermodynamic calculations can be performed using a database developed in the framework of the Pitzer model for activity coefficient correction

Preprints (www.preprints.org) | NOT PEER-REVIEWED | Posted: 9 September 2022 doi:10.20944/preprints202209.0138.v1

[13]. Such data have been recently improved [14, 15] but remain incomplete, especially to described all cementitious phases – and particularly uranium phases – under such extreme ionic strength.

The aim of this study is to determine the effect of high content of $NaNO_3$, up to 2.8 $mol/kg_{solution}$ onto the sorption of U(VI) in a hardened cement-paste (HCP). Because of high ionic strength and expected low solubility of uranium in such alkaline condition, the selected analytical method to measured accurate U(VI) concentration in solution is the time-resolved laser fluorescence (TRLFS) technique coupled to the method of standard addition. This technique has been proved particularly useful for speciation characterization of specific luminescent species in solution such as U(VI) [16], Cm(III) [17], or Eu(III) [18]. It can be used for quantitative determination as well [19-**Error! Reference source not found.**], using the method of standard addition to limit dilution factor and matrix effects.

2. Materials and Methods

2.1 Cement-based materials preparation and characterization

Cement-based materials have been prepared using a CEM I cement (CEM I 52.5N CE PM-ES-CP2 NF– Val d'Azergues, Lafarge). Cement paste samples were prepared with water to cement mass ratio, w/c, of 0.43. Ultrapure water (Merck Millipore Milli-Q, with a resistivity at 25°C of 18.2 MΩ.cm) has been used as water in this study. The cement samples were poured into closed cylindrical polyethylene plastic molds (125 cm^3) and initially cured at 100% relative humidity chamber for 28 days. After the curing period, hardened cement paste (HCP) samples were crushed, sieved (fraction < 250 µm) and kept under N_2 atmosphere in a glove box to avoid excess of carbonation (P_{CO2} < 1 ppm, CO_2 gas analyzer 410i model, MEGATEC).

The artificial cement porewater (S1-0-$NaNO_3$) is an alkaline solution, which was used to equilibrate all HCP samples during additional cure and retention experiments. The S1-0-$NaNO_3$ solution is a portlandite ($Ca(OH)_2$) saturated solution with (65 ± 2) 10^{-3} $mol/kg_{solution}$ of Na^+, (140 ± 2) 10^{-3} $mol/kg_{solution}$ of K^+ resulting to a pH value of (13.3 ± 0.1). pH value for the S1-0-$NaNO_3$ solution is determined using a PHM250 pHmeter (Radiometer Analytical) with a temperature probe and a combined pH glas electrode (Ag/AgCl, with KCl 3 $mol/kg_{solution}$ as electrolyte, Metrohm). Calibration was carried out using 3 Certipur buffer solutions (Merck) with theoretical pH values at 22°C of 7.01 (potassium dihydrogen phosphate and di-sodium hydrogen phosphate, KH_2PO_4/Na_2HPO_4 c.a. 0.020/0.0275 $mol/kg_{solution}$), 9.21 (borate solution, $Na_2B_4O_7$ à 0.01 $mol/kg_{solution}$), and 12.09 (di-sodium hydrogen phosphate, $Na_2HPO_4$and sodium hydroxide, NaOH in water). An alkaline solution (0.1 $mol/kg_{solution}$ NaOH) whose pH is 13.0 is used to check the linearity of the calibration above pH = 12.09. The pH measurements were made with an uncertainty calculated at 2σ or 0.1 pH unit. The chemicals used for the preparation of such a solution are NaOH (Sigma-Aldrich, CAS-N°: 1310-73-2), KOH (Emsure, Merck, CAS-N°: 1310-58-3), CaO (Sigma-Aldrich, CAS-N°: 1305-78-8). The S1-0-$NaNO_3$ solution is systematically filtered (Nylon, 0.45 µm, Nalgene) to remove the excess of portlandite before $NaNO_3$ addition and its use in retention experiments. The appropriate amount of $NaNO_3$ salt (AnalR Normapur, VWR, CAS-N°: 7631-99-4) was then added to the S1-0-$NaNO_3$ to reach 1.4 moles of $NaNO_3$ per kilogram of S1-0-$NaNO_3$ solution and 2.8 moles of $NaNO_3$ per kilogram of S1-0-$NaNO_3$ solution, the resulting solutions were labelled S1-1.4-$NaNO_3$ and S1-2.8-$NaNO_3$, respectively. The density of each resulting solution has been determined at 22°C using an electronic pycnometer (Mettler Toledo, densito-30PX) and a value of 1.0077, 1.0823 and 1.1541 g/cm^3 are obtained for S1-0-$NaNO_3$, S1-1.4-$NaNO_3$ and S1-2.8-$NaNO_3$, respectively. Calcium concentration after filtration has been determined in the meantime as the other major cations by ionic chromatography (IC, Metrohm, C3 column, HNO_3 5 10^{-3} $mol/kg_{solution}$ as eluent solution) for the S1-0-$NaNO_3$ solution and a value of (6 ± 1) 10^{-3} $mol/kg_{solution}$ is obtained. For the other solutions due to important $NaNO_3$ content, calcium concentration was not possible to be measured accurately by IC technique.

Preprints (www.preprints.org) | NOT PEER-REVIEWED | Posted: 9 September 2022 doi:10.20944/preprints202209.0138.v1

After this initial period of cure, the crushed HCP samples were maintained in the S1-x-$NaNO_3$ (x = 0, 1.4 and 2.8) solutions for 6 months to achieve a better hydration and reaction with $NaNO_3$ with a liquid/solid ratio of (27 ± 1) $kg_{solution}/kg_{solid}$. Solid was separated from solution by ultracentrifugation (Beckman 50 000 g, 1 hour) and dried overnight in a desiccator flushed with Ar. Solid samples were then characterized by X-ray diffractometry (XRD, INEL XRG 3000) using a Co anode as X-ray source (λ_{Co} = 1.7903 Å). Diffractogramms were then analyzed using the "Match !" (Phase identification from powder diffraction, Crystal impact, version 3) and the Crystallography open database (COD), http://www.crystallography.net/cod/.

2.2 Induced coupled plasma - mass spectrometry

Uranium concentration was determined by induced coupled plasma - mass spectrometry (ICP-MS 810-MS, AGILENT). To this aim, the cementitious samples were diluted in 2% HNO_3 solution (using HNO_3 65%, suprapur, Aldrich CAS-7697-37-2) with a dilution factor of 3000 in order to decrease the pH value and to minimize sodium content in the matrix. External calibration curve was measured using U(VI) diluted solutions in the range 10^{-11} $mol/kg_{solution}$ and 2.10^{-9} $mol/kg_{solution}$ prepared from uranium standard solution (1003 ± 4 $mg/kg_{solution}$ in 4% HNO_3 solution, plasmaCal, SCP science). A spike of a solution containing ^{208}Tl to reach 10^{-10} $mol/kg_{solution}$ was used to check the stability of the signal intensity.

2.3 Time-resolved laser fluorescence spectroscopy

The concentration of U(VI) was determined by time-resolved laser fluorescence (TRLFS) technique using the method of standard addition. The principles and TRLFS setup used in this study has already been fully described elsewhere [19-28]. Taking advantage of the time-resolution and the luminescence properties of U(VI) species in phosphoric media [19, **Error! Reference source not found.**] the luminescence spectra were obtained at λ_{exc} = 300 nm, at a delay D = 2 µs after the laser flash, during a gate width W = 1 ms, and accumulating 1000 spectra. The decomposition of the spectra were done using the Solver from Microsoft Excel as already explained elsewhere [24], and the fitting uncertainties and correlation matrices were calculated using the SolverAid macro [29]. For this study, and prior to the TRLFS characterization, an aliquot of 2 mL of the U(VI)-content cementitious solutions has been acidified with a spike of 120 µL of orthophosphoric acid (H_3PO_4, 85%, Merck CAS-N° 7664-38-2). Thus, the resulting pH value is closed to 2. For an initial U(VI) concentration of 5.10^{-6} mol/L in 0.8 mol/kg_w H_3PO_4 the following speciation is expected : 80% of $UO_2(H_2PO_4)_2$, 11% of $UO_2(H_2PO_4)(H_3PO_4)^+$ and 9% $UO_2(H_2PO_4)^+$. Figure 1 shows the TRLFS results obtained for such a solution. The luminescence spectrum shows typical fingerprint of uranyl species in acidic conditions. The lifetime decay evolution can be fitted with a mono-exponential curve and a lifetime τ = (164 ± 1) µs can be calculated from these data. This result suggests that only one species is observed and desexcitation processes of all other theoretical species are faster than what can be observed.

Preprints (www.preprints.org) | NOT PEER-REVIEWED | Posted: 9 September 2022 doi:10.20944/preprints202209.0138.v1

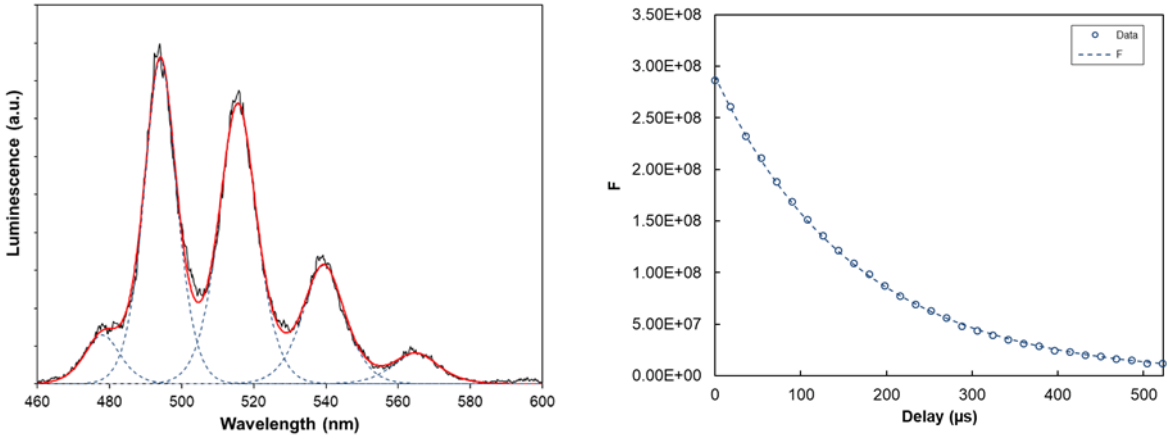

(**a**) (**b**)

Figure 1. TRLFS results obtained for a solution with an initial U(VI) concentration of 5.10^{-6} mol/L in 0.8 mol/kg_w H_3PO_4: (**a**) U(VI) luminescence spectrum in H_3PO_4 solution; (**b**) lifetime decay of the resulting U(VI) species.

2.4 U(VI) operational solubility determination

For each investigated cementitious solution and $NaNO_3$ content, the operational solubility of U(VI) has been investigated. A spike of the U(VI) standard solution is added to 25 mL of the cementitious solution to reach approximatively 10^{-4} mol/$kg_{solution}$ as initial concentration. A second spike of U(VI) standard solution is performed right after the first sampling to increase the initial concentration to 2 10^{-4} mol/$kg_{solution}$. After 24 h, a yellow-orange precipitate is observable in each solution. After 4 h, 48 h, and 7 months of contact time, the tubes are placed in an ultracentrifuge device (50 000 g, 1 h, Beckman) in order to separate the solid-precipitate from the solution. HNO_3 5% is added to acidify and dilute the two first samplings, then the U(VI) concentration is measured using an induced-coupled-plasma mass-spectrometer (ICP-MS, Agilent). The spike of H_3PO_4 85% solution is added to the last samplings and the U(VI) concentration is determined by the TRLFS technique coupled to the method of standard addition.

2.5 Batch sorption determination

In order to evaluate the effect of $NaNO_3$ onto U(VI) affinity for HCP, batch sorption experiments were performed on dispersed materials. All batch sorption experiments were carried out in polysulfone polymer (PSF) centrifuge tubes (Nalgene) with polypropylene screw closure. Batch sorption experiments were carried out using a diluted U(VI) standard solution. The solution-to-solid ratio is for each HCP suspensions and U(VI) initial concentration are given in Table 1.

Table 1. Initial conditions for U(VI) batch sorption as a function of $NaNO_3$ content.

	V/m [$kg_{solution}/kg_{solid}$]	**$[U(VI)]_{ini}$** [$mol/kg_{solution}$]
S1-0-$NaNO_3$	325 ± 19	$(9.2 \pm 1.5).10^{-7}$
S1-1.4-$NaNO_3$	346 ± 20	$(8.5 \pm 0.6).10^{-7}$
S1-2.8-$NaNO_3$	364 ± 12	$(7.3 \pm 1.1).10^{-7}$

Figure 2a corresponds to luminescence spectra obtained for the U(VI) blank solution in the S1-0-$NaNO_3$ solution in 0.8 mol/kg_w H_3PO_4 as a function of U(VI) standard addition. Figure 2b corresponds to the evolution of the intensity obtained for the fluorescence peak à 495 nm as a function of the U(VI) standard addition Data treatment leads to obtain a U(VI) concentration of (8.1 ± 1.3) 10^{-7} mol/$kg_{solution}$ which is consistent with the theoretical initial concentration of 9.2 10^{-7} mol/$kg_{solution}$ for this sample (see Table 1). For each initial

Preprints (www.preprints.org) | NOT PEER-REVIEWED | Posted: 9 September 2022 doi:10.20944/preprints202209.0138.v1

U(VI) concentration, the similar experimental determination by TRLFS has been performed (spectra not shown).

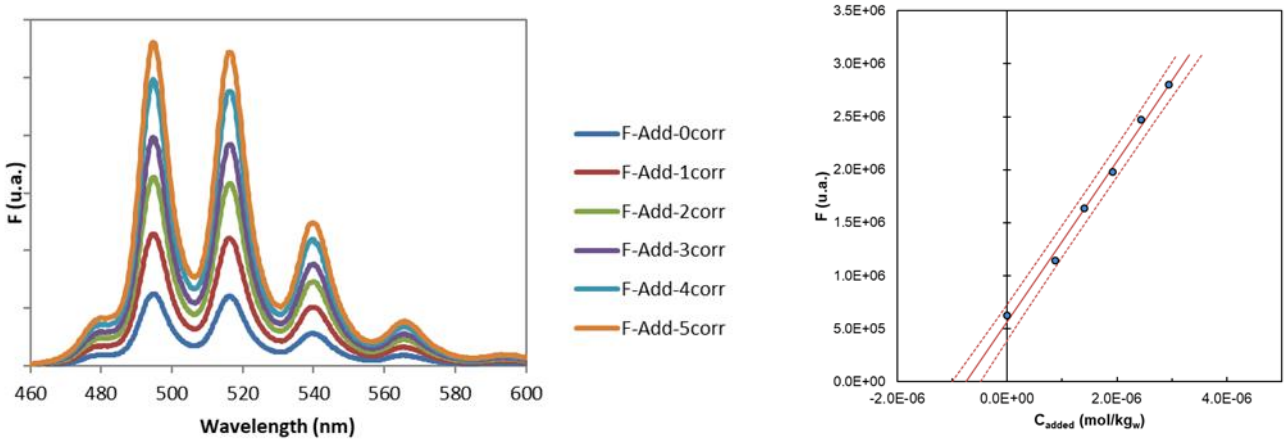

(**a**) (**b**)

Figure 2. Luminescence spectra of U(VI) in 0.8 mol/kg_w H_3PO_4 as a function of U(VI) standard addition: (**a**) raw U(VI) luminescence spectra; (**b**) evolution of the intensity obtained for the peak à 495 nm as a function of the U(VI) standard addition.

Experimental results are expressed as distribution ratio (R_d) in $kg_{solution}/kg_{solid}$, which correspond to the distribution of U(VI) between its concentration in the solid ($[U(VI)]_{solid}$) and the one in solution ($[U(VI)]_{solution}$) as defined by Eq.1.

$$R_d = \frac{[U(VI)]_{solid}}{[U(VI)]_{solution}} = \frac{([U](VI)_{ini} - [U(VI)]_{solution})}{[U(VI)]_{solution}} \times \frac{V}{m} \quad (1)$$

$[U(VI)]_{ini}$ (mol/$kg_{solution}$) is the introduced concentration; V ($kg_{solution}$) is the volume of solution and m (kg_{solid}) is the calculated dry mass of solid. $[U(VI)]_{ini}$ (mol/$kg_{solution}$) is determined either by ICP-MS and TRLFS measurements from a "blank sample", which was similarly prepared without cementitious materials. $[U(VI)]_{solution}$ (mol/$kg_{solution}$) is the concentration of U(VI) in the supernatant measured after 1, 8, and 15 days by ICP-MS and after 1 month of contact time by TRLFS using the method described in this paper.

After 1 month of contact time with U(VI), the suspensions were ultracentrifuged (at 50 000 g for 1 hour, Beckmann) before removing completely the supernatant. The residual amount of U(VI) in the supernatant after sorption was determined by TRLFS using the method described in this paper.

To quantify desorption, the supernatant is replaced by the equivalent volume of cementitious solution containing the same amount of $NaNO_3$. The value of the R_d after desorption is then calculated as in Eq.1, where $[U(VI)]_{ini}$ (mol/$kg_{solution}$) is calculated from the sorption result and correspond to the U(VI) species present in the solid by sorption and in the residual solution after separation; and $[U(VI)]_{solution}$ (mol/$kg_{solution}$) is the concentration of U(VI) in the supernatant measured by TRLFS after 1 month of contact time of desorption.

The batch sorption/ desorption experiments were carried out in a glove box with $P(CO_2) < 1$ ppm to avoid sample alteration by atmospheric carbonation.

3. Results

 doi:10.20944/preprints202209.0138.v1

3.1 Evolution of the cementitious-phases assembly as a function of $NaNO_3$ content

Figure 3 represents the evolution of the cementitious-phases assembly as a function of $NaNO_3$ content and after 6 months of contact time. The experimental pattern of the sample containing no $NaNO_3$ (series labelled "NaNO3 0M BIS" in Figure 3) corresponds to a classic-CEM I-hydrated-cement-paste assembly containing ettringite ($Ca_6Al_2(SO_4)_3(OH)_{12}(H_2O)_{26}$, COD ref [00-041-1451]), portlandite ($Ca(OH)_2$, COD ref [00-044-1481]) and some amorphous phases supposed to correspond to calcium silicate hydrate phases (CSH) in the 2θ regions between 5°-10° and between 30°-45°. Peaks corresponding to the calcite ($CaCO_3$, COD ref [00-083-1762]) have been added to the pattern because its presence in the assembly is suspected but not fully proved because of the lack of the main peak at 2θ ca. 34.3°. The XRD result obtained for the sample cured in contact with 1.4 $mol/kg_{solution}$ $NaNO_3$ (series labelled "NaNO3 1,4M BIS" in Figure 3) and 2.8 $mol/kg_{solution}$ $NaNO_3$ (series labelled "NaNO3 2,8M BIS" in Figure 3) show a similar diffractogram. In addition, nitratine corresponding to a crystallized sodium nitrate phase ($NaNO_3$, COD ref [00-036-1474]) and darapskite, which corresponds to a nitrate sulfate hydrate phase ($Na_3(NO_3)(SO_4)(H_2O)$, COD ref [00-074-1238]) are also observed. The presence of nitratine could be explained by sample preparation before XRD acquisition. As the HCP sample dried in desiccator without any rinsing procedure, some residual curing solution containing a significant amount of $NaNO_3$ may precipitate and crystallize during the drying time. Without sulfate ions in solution, the precipitation of $NaNO_3$ is expected for concentrations higher than 10 mol/kg_w (*Cf.* [30]).

As far as no internal XRD standard was mixed with the HCP powder, the diffractogram can only be interpreted qualitatively. Nevertheless, the decrease of the main portlandite peak is observed when $NaNO_3$ content is increasing. This observation could be linked to an increase of portlandite solubility with increasing $NaNO_3$ content [9,31]. Moreover, for the samples cured in contact with $NaNO_3$, the 2θ region between 8° and 12° shows the occurrence of darapskite, which is correlated with the decreasing of the main peak of ettringite. This darapskite crystalline phase has already been observed in cement based materials in literature [10], and its formation could be explained by the presence of sulfate in solution after ettringite dissolution. In this study, no particular effort has been made to simulate by thermodynamic calculations the observed concentrations in solution compared to the cementitious assembly in the solid. This is due to (i) a lack of thermodynamic data on cementitious phases within the framework of the Pitzer model [13, 32]; and (ii) the too high solubility of both nitratine and darapskite to be accurately modelled in the framework of the specific ion interaction theory (SIT) – see Annex B in Guillaumont *et al*. [2].

Preprints (www.preprints.org) | NOT PEER-REVIEWED | Posted: 9 September 2022 doi:10.20944/preprints202209.0138.v1

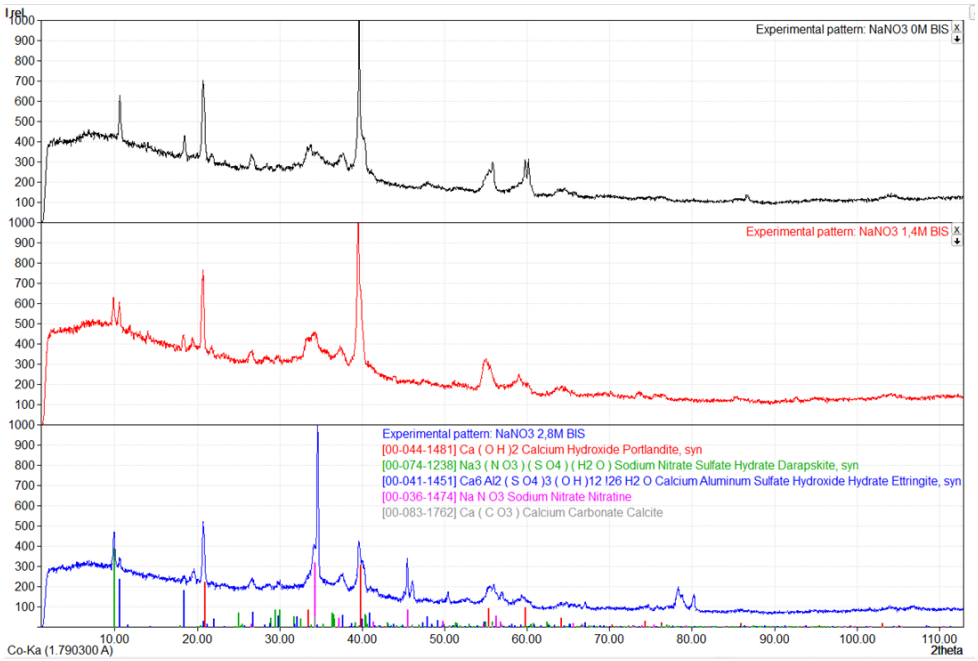

Figure 3. XRD patterns of CEM I HCP samples powder after 6 months of equilibration in $NaNO_3$ cementitious solutions.

3.2 Evolution of the U(VI) solubility limit as a function of $NaNO_3$ content

Table 2 corresponds to the measured U(VI) concentration after 4 h, 48 h, and 7 months of contact time.

After 4 h of contact time, the remaining concentration is comparable to the initial one (*i.e.* 10^{-4} mol/$kg_{solution}$) with respect of experimental uncertainties. The second spike of U(VI) (*i.e.* $[U(VI)]_{initial} = 2.10^{-4}$ mol/$kg_{solution}$) leads to the formation 24 h later of a yellow-orange precipitate in each system. After 48 h of contact time, the U(VI) concentration in solution decreased to a minimum of $(1.67 \pm 0.03)\ 10^{-5}$ mol/$kg_{solution}$ for the system with the higher amount of $NaNO_3$. After 48 h of contact time and for the S1-0-$NaNO_3$ system, the U(VI) concentration is higher with a factor of *ca*. 5, compared to the systems with $NaNO_3$. This gap decreases to a factor *ca*. 3 after 7 months of contact time.

Table 2. U(VI) concentration measured in solution as a function of contact time and $NaNO_3$ content.

	S1-0-$NaNO_3$ [mol/$kg_{solution}$]	**S1-1.4-$NaNO_3$ [mol/$kg_{solution}$]**	**S1-2.8-$NaNO_3$ [mol/$kg_{solution}$]**
4 h, ICP-MS	$(1.1 \pm 0.1)\ 10^{-4}$	$(9.6 \pm 0.5)\ 10^{-5}$	$(1.0 \pm 0.1)\ 10^{-4}$
48 h, ICP-MS	$(8.68 \pm 0.08)\ 10^{-5}$	$(1.38 \pm 0.03)\ 10^{-5}$	$(1.67 \pm 0.03)\ 10^{-5}$
7 m, ICP-MS	<LOD	<LOD	<LOD
7 m, TRLFS	$(7.2 \pm 2.1)\ 10^{-6}$	$(2.7 \pm 0.3)\ 10^{-6}$	$(2.2 \pm 0.4)\ 10^{-6}$

Based onto a PHREEQC calculation [32] using the Thermochimie database [34] and the specific interaction theory as model for activity coefficient correction, a theoretical speciation for U(VI) in the S1-0-$NaNO_3$ system shows $UO_2(OH)_3^-$ and $UO_2(OH)_4^{2-}$ as main aqueous species.

The operational solubility measured elsewhere [4, 35, 36] is close to 10^{-7}-10^{-5} mol/$kg_{solution}$ for solution with an ionic strength up to < 0.5 mol/$kg_{solution}$. In these studies, the amount of precipitate was not sufficient to perform a solid characterization. The orange-yellow precipitate is typical to U(VI)-content solid in such conditions is currently reported by literature – see *e.g.* ref. [3]. The $CaUO_4.xH_2O$ phase appears as the best candidate to explain the solubility limit in S1-0-$NaNO_3$-type solution, in reference to spectroscopic evidences [3]. Solubility constant of the hydrated calcium uranate is not available

Preprints (www.preprints.org) | NOT PEER-REVIEWED | Posted: 9 September 2022 doi:10.20944/preprints202209.0138.v1

in literature. One can estimate it using solubility constant of $CaUO_{4(cr)}$ from Grenthe *et al.* [37] .Best option could be the use of the solubility constant of $CaU_2O_7{:}3H_2O_{(cr)}$ from Altmaier *et al.* [5]. Taking into consideration the $CaU_2O_7{:}3H_2O$ as only U(VI)-solubility-limiting phase, adding 10^{-4} mol/$kg_{solution}$ of uranyl in the S1-0-$NaNO_3$ solution lead to reach a residual uranyl concentration of 6.10^{-6} mol/$kg_{solution}$, which is consistent with what was obtained after 7 months of equilibration. Other PHREEQC calculations were performed using $CaU_2O_7{:}3H_2O$, $K_2U_2O_7{:}1.5H_2O$,and $Na_2U_2O_7{:}H_2O$ as U(VI)-solubility-limiting-phase candidates : with an initial U(VI) concentration of 10^{-4} mol/$kg_{solution}$, the increase of $NaNO_3$ up to 2.8 mol/$kg_{solution}$ leads to decrease the U(VI) concentration to 9.10^{-7} mol/$kg_{solution}$, when $Na_2U_2O_7{:}H_2O$ is the major phase responsible to limit the solubility of U(VI).

Figure 4a corresponds to luminescence spectra of U(VI) species present in the supernatant after 7 months of contact time in contact with $NaNO_3$ with a spike of H_3PO_4, 85%. The spectra have been normalized with respect to the U(VI) concentration determined after U(VI) standard addition. It seems that the addition of $NaNO_3$ until 1.4 mol/$kg_{solution}$ increase the intensity of U(VI) in phosphoric media, then the opposite trend is observed. The inflection point of this trend cannot be determined only with these result. Figure 4b corresponds to the same spectra normalized by the total area of each spectrum. This representation allows to conclude that the same speciation is observed in all investigated media after the addition of the spike of H_3PO_4, 85%.

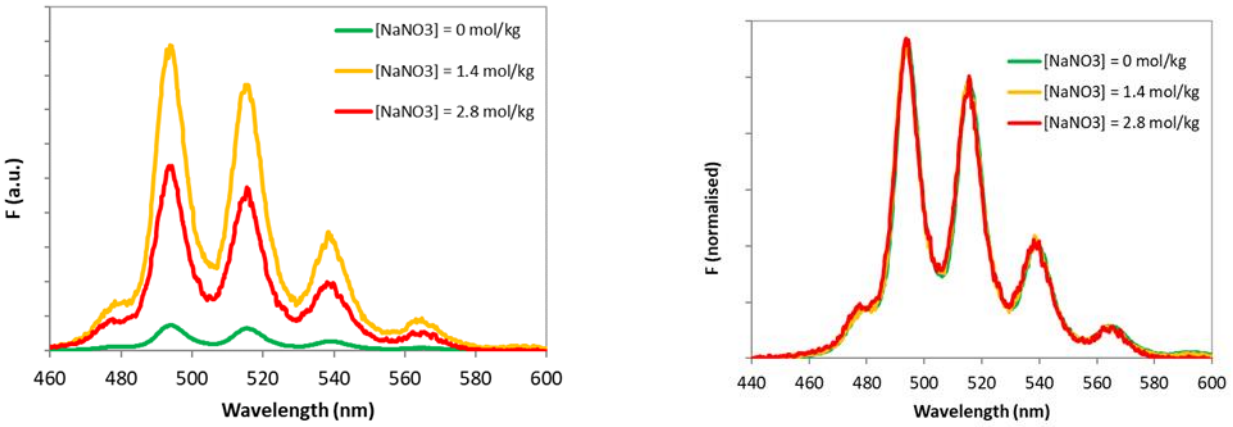

(**a**) (**b**)

Figure 4. Luminescence spectra of U(VI) in 0.8 mol/kg_w H_3PO_4 and as a function of $NaNO_3$ content: (**a**) luminescence spectra normalized considering the U(VI) concentration; (**b**) U(VI) luminescence spectra normalized to the area of the spectra.

The initial U(VI) concentration in batch sorption experiments given in Table 1 has been chosen taking into consideration the operational solubility limit. This allows avoiding the U(VI) precipitation. Then, the decrease of U(VI) concentration in solution after contact with the HCP can be attributed only to sorption phenomena.

3.3 U(VI) retention onto hardened cement paste under high saline and alkaline conditions

No accurate U(VI) species fluorescence spectra were obtained in supernatant after investigated contact times in HCP suspensions . Because of the amount of $NaNO_3$ in the alkaline supernatant, the spectra acquired at ambient temperature presents no clear uranyl-fingerprint-shape for all samples. Note that the $UO_2(OH)_4^{2-}$ species was observed only at 153 K by Tits *et al.* [37]. The addition of high amount of $NaNO_3$ decreases the intensity of the signal, suggesting a high matrix effect onto the fluorescence in such media.

Figure 5 represents the sorption kinetics obtained as a function of $NaNO_3$ content. Results are expressed in R_d values. Contact times are ranging from 1 days to 30 days before U(VI) concentration measurement and R_d determination. Due to analytical issues, in the S1-0-$NaNO_3$ system, only the sample after 30 days of contact time was determined. For

Preprints (www.preprints.org) | NOT PEER-REVIEWED | Posted: 9 September 2022 doi:10.20944/preprints202209.0138.v1

the other systems, U(VI) concentration in the supernatant was determined for each contact time. There is almost a factor 4 between R_d values at high $NaNO_3$ content and the one obtained in the reference system. The R_d value obtained after 30 days of contact time in the reference system is similar to those reported in literature for comparable cementitious-system [1]. There is not a clear trend of the evolution of R_d value with time, taking into consideration the experimental uncertainties. This result suggest that equilibrium is reached at the latest after 30 days of contact time. A fast sorption mechanism can be considered in these media, as previously observed [35, 36], where a steady-state was attained within *ca*. 15 days.

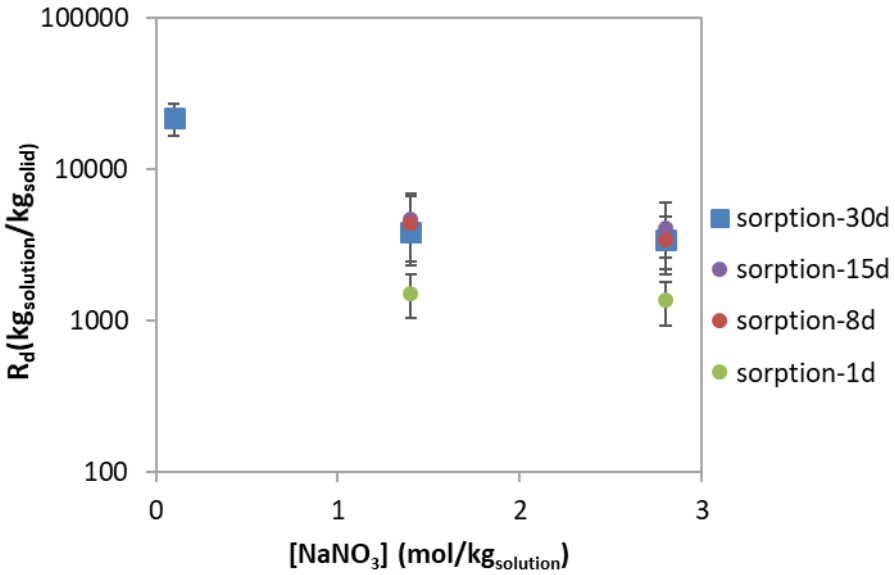

Figure 5. U(VI) sorption kinetics as a function of $NaNO_3$ content.

The decrease of R_d values with increasing ionic strength are consistent with R_d values recommended by Ochs et al. [39] in presence of high ionic strength, in NaCl media up to 6 M.

Table 3 and Figure 6 represent data obtained for sorption and desorption after 30 days of contact time. Considering experimental uncertainties, the U(VI) concentration in supernatant after desorption is comparable to the one obtained after sorption for each system. In Figure 7, the R_d values for sorption and desorption are comparable. A higher value is observed for the reference system for sorption and desorption. From these results, one can conclude that a reversible U(VI) sorption mechanism occurs in all investigated systems, despite of the $NaNO_3$ content.

Table 3. U(VI) concentration measured by TRLFS in supernatant after 1 month of sorption or desorption as a function of $NaNO_3$ content.

	S1-0-$NaNO_3$ [$mol/kg_{solution}$]	**S1-1.4-$NaNO_3$ [$mol/kg_{solution}$]**	**S1-2.8-$NaNO_3$ [$mol/kg_{solution}$]**
sorption	$(1.3 \pm 0.1)\ 10^{-8}$	$(7.4 \pm 1.2)\ 10^{-8}$	$(6.8 \pm 0.8)\ 10^{-8}$
desorption	$(1.6 \pm 0.3)\ 10^{-8}$	$(5.9 \pm 1.6)\ 10^{-8}$	$(4.6 \pm 0.9)\ 10^{-8}$

Preprints (www.preprints.org) | NOT PEER-REVIEWED | Posted: 9 September 2022 doi:10.20944/preprints202209.0138.v1

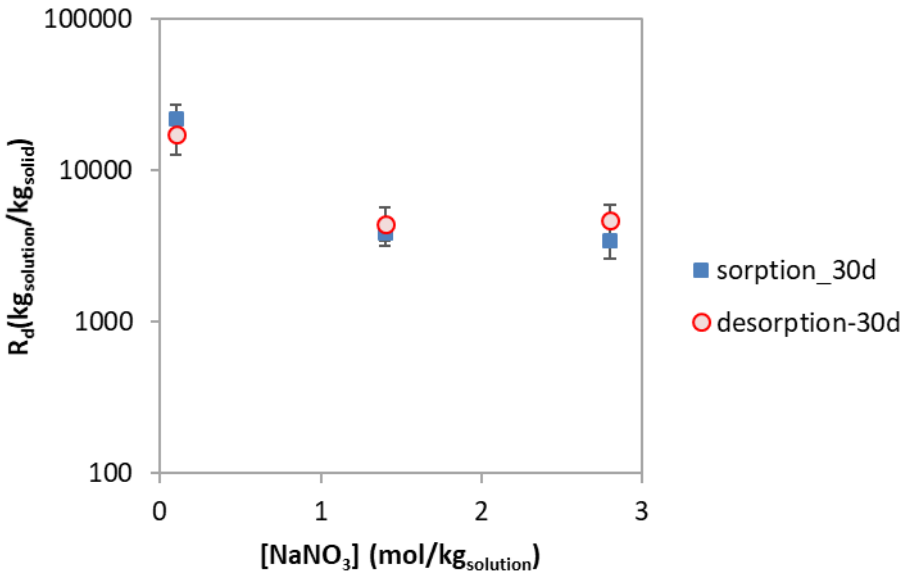

Figure 6. U(VI) sorption and desorption after 30 days of contact time as a function of $NaNO_3$ content.

4. Conclusions

Our aim was to study the influence of a saline plume on the U(VI) retention onto cementitious phases. The use of standard addition method – in H_3PO_4 85% – in TRLFS allowed us to (i) circumvent the high matrix effects of up to 2.8 $mol/kg_{solution}$ $NaNO_3$ media; (ii) drastically limit dilution factor; and (iii) determine the resulting [U(VI)] in solution with acceptable precision for distribution factor (R_d) determination in sorption and desorption experiments. The R_d values decrease by a factor *ca.* 4 with the decrease by a factor 3 of operational solubility limit measured at high ionic strength compared to the reference cementitious condition. The sorption of U(VI) appears to be reversible. Mineralogical phase assembly observed for the HCP after curing in $NaNO_3$ solutions cannot directly be linked to the decrease of R_d values. There is still a need to verify the affinity of uranium for each observed cementitious individual phases to obtain a comprehensive overview of the system, with a particular attention to calcium silicate hydrates and AFm/AFt phases.

Author Contributions: Formal analysis, J.P., N.M., P.E.R., methodology, N.M., P.E.R.; investigation, N.M., P.E.R.; writing—original draft preparation, N.M.; writing—review and editing, N.M., P.E.R.; supervision, N.M., P.E.R. All authors have read and agreed to the published version of the manuscript.

Data Availability Statement: Not Applicable.

Acknowledgments: This work received financial support from the French National Agency for Radioactive Waste Management (Andra). The authors acknowledge Dr. P. Henocq for fruitful discussions.

Conflicts of Interest: The authors declare no conflict of interest.

References

1. Ochs, M.; Mallants, D.; Wang, L. *Radionuclide and metal sorption on cement and concrete. Topics in safety, Risk, reliability and Quality*, Springer. ed. Springer International Publishing, Switzerland, 2016.

2. Guillaumont, R.; Fanghänel, T.; Neck, V.; Fuger, J.; Palmer, D.A.; Grenthe, I.; Rand, M.H. *Update on the chemical thermodynamics of uranium, neptunium, plutonium, americium and technetium, Chemical thermodynamics*. Elsevier ; Nuclear Energy Agency; Organisation for Economic Co-Operation and Development; Amsterdam ; Boston : Paris; 2003, pp 919.

3. Macé, N.; Wieland, E.; Dähn, R.; Tits, J.; Scheinost, A.C. EXAFS investigation on U(VI) immobilization in hardened cement paste: influence of experimental conditions on speciation. *Radiochimica Acta* **2013**, 101, 379–389. DOI: 10.1524/ract.2013.2024.

4. Wieland, E.; Macé, N.; Dähn, R.; Kunz, D.; Tits, J. Macro- and micro-scale studies on U(VI) immobilization in hardened cement paste. *Journal of Radioanalytical and Nuclear Chemistry* **2010**, 286, 793–800. DOI: 10.1007/s10967-010-0742-y.

5. Altmaier, M., Neck, V., Mueller, R., Fanghänel, T. Solubility of U(VI) and formation of $CaU_2O_7{:}3H_2O$(cr) in alkaline $CaCl_2$ solutions. MIGRATION 2005, 10th international conference on chemistry and migration behaviour of actinides and fission products in the geosphere, 18-23 Sept 2005. Avignon, France. http://inis.iaea.org/search/search.aspx?orig_q=RN:38061332

6. Altmaier, M.; Yalçıntaş, E.; Gaona; X.; Neck, V.; Müller, R.; Schlieker, M.; Fanghänel, T. Solubility of U(VI) in chloride solutions. I. The stable oxides/hydroxides in NaCl systems; solubility products; hydrolysis constants and SIT coefficients. *The Journal of Chemical Thermodynamics* **2017**, 114, 2–13, DOI: 10.1016/j.jct.2017.05.039.

7. Çevirim-Papaioannou, N.; Yalçıntaş, E.; Gaona, X.; Altmaier, M.; Geckeis, H. Solubility of U(VI) in chloride solutions. II. The stable oxides/hydroxides in alkaline KCl solutions: Thermodynamic description and relevance in cementitious systems. *Applied Geochemistry* **2018**, 98, 237–246, DOI: 10.1016/j.apgeochem.2018.09.017.

8. Endrizzi, F.; Gaona, X.; Zhang, Z.; Xu, C.; Rao, L.; Garcia-Perez, C.; Altmaier, M. Thermodynamic description of U(VI) solubility and hydrolysis in dilute to concentrated NaCl solutions at T = 25; 55 and 80°C. *Radiochimica Acta* **2019**, 107, 663–678, DOI: 10.1515/ract-2018-3056.

9. Johnston, J.; Grove, C. The solubility of calcium hydroxide in aqueous salt solutions; *Journal of the American Chemical Society*; **1931**, 53, 3976–3991. DOI: 10.1021/ja01362a009.

10. Malone, P.G.; Poole, T.S.; Wakeley, L.D.; Burkes, J.P. Salt related expansion reactions in Portland-cement-based wasteforms. *Journal of Hazardous Materials*; **1997**, 52, 237–246. DOI: 10.1016/S0304-3894(96)01810-9.

11. Liu, L.; Sun, C.; Geng, G.; Feng, P., Li, J., Dähn, R. Influence of decalcification on structural and mechanical properties of synthetic calcium silicate hydrate (C-S-H). *Cement and Concrete Research* **2019**, 123, 105793. DOI: 10.1016/j.cemconres.2019.105793.

12. Zheng, Z.; Li, Y.; Yang, J.; Cui, M.; Wang, H.; Ma, X. Insights into the deterioration of C-S-H gels in hardened cement pastes with different $NaNO_3$ concentrations. *Construction and Building Materials* **2020**, 259, 120423. DOI: 10.1016/j.conbuildmat.2020.120423.

13. Pitzer, K. S. Activity Coefficients in Electrolyte Solutions, **1991**, CRC Press, Boca Raton, USA. pp. 542.

14. Lach, A.; André, L.; Lassin, A. Darapskite solubility in basic solutions at 25°C: A Pitzer model for the $Na\ NO_3SO_4OH\ H_2O$ system. *Applied Geochemistry*; **2017**, 78, 311–320. DOI: 10.1016/j.apgeochem.2016.12.008.

15. Reynolds, J.G.; Carter, R. A sulfate and darapskite solubility model with Pitzer interaction coefficients for aqueous solutions containing $NaNO_2$, $NaNO_3$, and NaOH. *The Journal of Chemical Thermodynamics* **2016**, 101, 380–386. DOI: 10.1016/j.jct.2016.06.027.

16. Shang, C., Reiller, P. E. Effect of temperature on the complexation of triscarbonatouranyl(VI) with calcium and magnesium in NaCl aqueous solution, *Dalton Transactions* **2021**, 50, 17165-17180. DOI: 10.1039/d1dt03204f.

17. Tits, J., Stumpf, T., Rabung, T., Wieland, E., Fanghänel, T. Uptake of Cm(III) and Eu(III) by calcium silicate hydrates: A solution chemistry and time-resolved laser fluorescence spectroscopy study, *Environmental Science & Technology* **2003** 37, 3568-3573. DOI: 10.1021/es030020b.

18. Huclier-Markai, S., Mazza, M., Alliot, C., Reiller, P. E. Luminescence spectroscopic investigations of europium(III) complexation with exopolysaccharides from a marine bacterium, *Dalton Transactions* **2021**, 50, 17215-17227. DOI: 10.1039/d1dt03288g.

19. Mauchien, P. Dosage de l'uranium par spectrofluorimétrie à source d'excitation laser; *CEA report* **1985**, CEA-R-5300, CEA, Fontenay-aux-Roses, France.

20. Berthoud, T.; Decambox, P.; Kirsch, B.; Mauchien, P.; Moulin, C. Direct uranium trace analysis in plutonium solutions by time-resolved laser-induced spectrofluorometry. *Analytical Chemistry* **1988**, 60, 1296–1299, DOI: 10.1021/ac00164a011.

21. Moulin, C.; Beaucaire, C.; Decambox, P.; Mauchien, P. Determination of uranium in solution at the ng l^{-1} level by time-resolved laser-induced spectrofluorimetry: application to geological samples. *Analytica Chimica Acta*; **1990**, 238, 291–296. DOI: 10.1016/S0003-2670(00)80550-4.

22. Decambox, P.; Mauchien, P.; Moulin, C. Direct and fast determination of uranium in human urine samples by laser-induced time-resolved spectrofluorometry. *Applied Spectroscopy;* **1991**, 45, 116–118, DOI: 10.1366/0003702914337768.

23. Reiller, P.; Lemordant, D.; Moulin, C.; Beaucaire, C. Dual use of micellar-enhanced ultrafiltration and time-resolved laser-induced spectrofluorimetry for the study of uranyl exchange at the surface of alkylsulfate micelles. *Journal of Colloid and Interface Science* **1994**, 163, 81–86. DOI: 10.1006/jcis.1994.1082.

24. Brevet, J., Claret, F., Reiller, P. E.; Spectral and temporal luminescent properties of Eu(III) in humic substance solutions from different origins, *Spectrochimica Acta Part A: Molecular and Biomolecular Spectroscopy*; **2009**, 74, 446-453. DOI:10.1016/j.saa.2009.06.042.

25. Kouhail, Y.Z.; Benedetti, M.F; Reiller, P.E. Eu(III)–fulvic acid complexation: evidence of fulvic acid concentration dependent interactions by time-resolved luminescence spectroscopy. *Environmental Science & Technology*; **2016**, 50, 3706–3713. DOI: 10.1021/acs.est.5b05456.

26. Reiller, P. E., Fromentin, E., Ferry, M., Dannoux-Papin, A., Badji, H., Tabarant, M., Vercouter, T. Complexing power of hydro-soluble degradation products from γ-irradiated polyvinylchloride: influence on $Eu(OH)_3(s)$ solubility and Eu(III) speciation in neutral to alkaline environment, *Radiochimica Acta*; **2017**, 105, 665-675. DOI: 10.1515/ract-2016-2691

27. Fromentin, E.; Reiller, P.E. Influence of adipic acid on the speciation of Eu(III): Review of thermodynamic data in NaCl and $NaClO_4$ media; and a new determination of Eu-adipate complexation constant in 0.5 $mol{\cdot}kg_w^{-1}$ $NaClO_4$ medium by time-resolved luminescence spectroscopy. *Inorganica Chimica Acta*; **2018**, 482, 588–596, DOI: 10.1016/j.ica.2018.06.035.

28. Kouhail, Y.Z.; Benedetti, M.F; Reiller, P.E. Formation of mixed Eu(III)-CO_3-fulvic acid complex: spectroscopic evidence and NICA-Donnan modeling. *Chemical Geology*, **2019**, 522, 175-185. DOI: 10.1016/j.chemgeo.2019.05.032.

29. De Levie; R. Advanced Excel for Scientific Data Analysis; Oxford University press, Oxford, USA, **2004**, pp 638.

30. Toghiani, R.K.; Phillips, V.A.; Smith, L.T.; Lindner, J.S. Solubility in the Na + SO_4 + NO_3 and Na + SO_4 + NO_2 systems in water and in sodium hydroxide solutions. *Journal of Chemical & Engineering Data* **2008**, 53, 798–804. DOI: 10.1021/je700666t.

31. Yeatts, L.B.; Marshall, W.L. Aqueous systems at high temperature. XVIII. Activity coefficient behavior of calcium hydroxide in aqueous sodium nitrate to the critical temperature of water. *The Journal of Physical Chemistry* **1967**, 71, 2641–2650. DOI: 10.1021/j100867a038.

32. Reardon, E. J. An ion interaction model for the determination of chemical equilibria in cement/water systems. *Cement and Concrete Research* **1990**, 20, 175-192. DOI: 10.1016/0008-8846(90)90070-e

33. Parkhurst, D.L.; Appelo, C.A.J. *User's guide to PHREEQC (version 2) - a computer program for speciation, batch-reaction, one-dimensional transport, and inverse geochemical calculations* Rapport U.S. Geological Survey No. Water-Resources Investigations, 99-4259). Lakewood, Colorado (U.S.A), 1999.

34. Giffaut, E.; Grivé, M.; Blanc, P.; Vieillard, P.; Colàs, E.; Gailhanou, H.; Gaboreau, S.; Marty, N.; Madé, B.; Duro, L. Andra thermodynamic database for performance assessment: ThermoChimie. *Applied Geochemistry* **2014,** 49, 225–236. DOI: 10.1016/j.apgeochem.2014.05.007.

35. Pointeau, I.; Landesman, C.; Giffaut, E.; Reiller, P. Reproducibility of the uptake of U(VI) onto degraded cement pastes and calcium silicate hydrate phases. *Radiochimica Acta* **2004,** 92. DOI:10.1524/ract.92.9.645.55008.

36. Tits, J.; Fujita, T.; Tsukamoto, M.; Wieland, E. Uranium(VI) uptake by synthetic calcium silicate hydrates. *MRS Proceedings* **2008**, 1107, 467–474. DOI: 10.1557/PROC-1107-467.

37. Grenthe, I., Gaona, X., Plyasunov, A. V., Rao, L., Runde, W. H., Grambow, B., Konings, R. J. M., Smith, A. L., Moore, E. E. **2020**. Second update on the chemical thermodynamics of Uranium, Neptunium, Plutonium, Americium and Technetium. NEA-OECD Chemical thermodynamics 14.

38. Tits, J.; Geipel, G.; Macé, N.; Eilzer, M.; Wieland, E. Determination of uranium(VI) sorbed species in calcium silicate hydrate phases: A laser-induced luminescence spectroscopy and batch sorption study. *Journal of Colloid and Interface Science* **2011**, 359, 248–256. DOI: 10.1016/j.jcis.2011.03.046.

39. Ochs, M.; Vriens, B.; Tachi, Y. Retention of uranium in cement systems: effects of cement degradation and complexing ligands. *Progress in Nuclear Science and Technology* **2018**, 5, 208–212. DOI: 10.15669/pnst.5.208.